Comparison of frozen-density embedding and discrete reaction field solvent models for molecular properties†

Christoph R. Jacob,*[a] Johannes Neugebauer,[a] Lasse Jensen[b] and Lucas Visscher*[a]

Received 10th February 2006, Accepted 4th April 2006
First published as an Advance Article on the web 20th April 2006
DOI: 10.1039/b601997h

We investigate the performance of two discrete solvent models in connection with density functional theory (DFT) for the calculation of molecular properties. In our comparison we include the discrete reaction field (DRF) model, a combined quantum mechanics and molecular mechanics (QM/MM) model using a polarizable force field, and the frozen-density embedding (FDE) scheme. We employ these solvent models for ground state properties (dipole and quadrupole moments) and response properties (electronic excitation energies and frequency-dependent polarizabilities) of a water molecule in the liquid phase. It is found that both solvent models agree for ground state properties, while there are significant differences in the description of response properties. The origin of these differences is analyzed in detail and it is found that they are mainly caused by a different description of the ground state molecular orbitals of the solute. In addition, for the calculation of the polarizabilities, the inclusion of the response of the solvent to the polarization of the solute becomes important. This effect is included in the DRF model, but is missing in the FDE scheme. A way of including it in FDE calculations of the polarizabilities using finite field calculations is demonstrated.

1. Introduction

Since properties and reactions of molecules are usually studied in solution, and since the solvent might not be innocent in experimental studies, there has been a growing interest in including solvent effects in theoretical investigations (for reviews, see, *e.g.*, ref. 1 and 2). Many solvent models used in quantum chemical studies are developed and well-tested for reproducing solvation energies or reaction energies in solution.[3–5] In some solvent models, only an (interaction) energy term is added so that effects on molecular properties cannot be described, apart from changes in the equilibrium structure. But modeling solvent effects on molecular properties has also attracted considerable attention during the past years, and several models for the inclusion of solvent effects on a more fundamental level have been proposed and tested (see, *e.g.*, ref. 6–21).

The models for the description of solvation effects can be divided into two groups. In continuum solvation models[1,2,22] the solvent is described as a continuous medium that is characterized by its dielectric constant, with the solute molecule residing inside a cavity in this medium. The solute molecule can then be treated with different quantum mechanical (QM) methods. Since the atomistic structure of the solvent is not explicitly included in these continuum models, the averaging over different solvent configurations is implicitly included in the continuum description that is parameterized to include all the degrees of freedom of the solvent. While it is clear that continuum models are able to correctly describe non-specific solvation effects, *i.e.*, dielectric medium effects, their ability to describe specific interactions like hydrogen bonding is less obvious. Although progress in this direction has been made, a description of specific interactions within continuum models apparently requires a very careful parameterization of the size and shape of the cavity in which the solute molecule is placed.[5]

A physically more appealing approach to the description of specific solvent effects is given by discrete solvent models in which the geometrical structure of the solvent is explicitly included. This offers a more straightforward way to take specific interactions into account. However, to provide a complete description of all solvation effects in discrete models it is necessary to average over the degrees of freedom of the solvent. This can be achieved by sampling over a large number of snapshots from classical[23] or Car–Parinello molecular dynamics (CPMD)[24,25] simulations. For all these solvent structures, the molecular properties of interest are then calculated using QM methods, taking the (discrete) solvent into account in a cluster model.[10,12] This can, for instance, be done using density functional theory (DFT)[26] for ground state properties or time-dependent DFT (TDDFT)[27,28] for response properties. Finally, the calculated property is averaged over the ensemble of solvent structures. This approach is denoted as ''sequential molecular dynamics followed by quantum mechanics calculations'' (S-MD/QM) following the terminology

[a] *Vrije Universiteit Amsterdam, Department of Theoretical Chemistry, Faculty of Sciences, De Boelelaan 1083, 1081 HV Amsterdam, The Netherlands. E-mail: jacob@few.vu.nl; jneugeb@chem.vu.nl; visscher@chem.vu.nl*
[b] *Northwestern University, Department of Chemistry, 2145 Sheridan Road, Evanston, IL 60208-3113, USA. E-mail: l.jensen@chem.northwestern.edu*

† Electronic supplementary information (ESI) available: Coordinates of the water cluster used in the calculations. See DOI: 10.1039/b601997h

of Canuto *et al.*[12] It usually requires the inclusion of a large number of solvent molecules in the solvent structures, which makes it necessary to use very efficient methods for the calculation of molecular properties.

The most accurate approach would be the calculation of the properties of interest from supermolecular calculations by using a sufficiently large cluster (if no periodic boundary conditions can be used) in the quantum chemical calculation. However, this approach is usually very demanding, since a large number of solvent molecules has to be included, which quickly becomes infeasible for large solutes. In addition, the supermolecular approach does not directly yield molecular properties of the solute. Analysis of the results requires some partitioning of the wave function that is usually not unique so the calculated molecular properties will strongly depend on the partitioning scheme used.[29]

More efficient, though more approximate approaches are combined quantum mechanics and molecular mechanics (QM/MM) models[30–34] in which only the solute is treated using QM methods, while molecular mechanics methods (MM) are used to describe the solvent as well as the interactions between solute and solvent. The restriction of the QM treatment to the solute system makes the calculation of molecular properties for a large number of structures feasible. However, the force field used in the MM part has to be parameterized carefully to describe the solute–solvent interactions accurately. In addition, QM effects on these interactions, which are important in the inner solvent shell, can only be modeled indirectly in an empirical way, even though there are studies that claim that carefully parameterized QM/MM models can yield results that are more reliable than DFT calculations.[35] For the calculation of response properties, it has been noted that it is necessary to use a polarizable MM model in which the solute can respond to charge redistribution in the solute.[36] One example of such a polarizable QM/MM scheme is the discrete reaction field (DRF) model,[7,8,37] which has been implemented within DFT for ground state[8] and response properties.[9] The DRF model has been previously applied to the calculation of molecular (hyper-)polarizabilities and of nonlinear optical (NLO) properties in solution.[38–40]

Frozen-density embedding (FDE)[41,42] within DFT can be regarded as a compromise between explicit QM models based on supermolecular cluster calculations and solvent treatments based on effective solvent–solute interaction potentials as used in DRF. In the FDE scheme, the (frozen) electron density of the solute is used to construct an embedding potential that enters in the calculation of the solute properties. The whole system (solute and solvent) is treated at a QM level, but the electron density of the solute and the solvent subsystems are determined separately. The calculation of orbitals for the supersystem is thus avoided. Even though FDE is in principle exact, further approximations—in addition to those present in conventional Kohn–Sham (KS) DFT—have to be introduced. For modeling solvation effects, FDE is usually combined with a simplified method for constructing the electron density of the solvent, *e.g.*, a sum-of-molecular-fragments approach.[15] Since the calculation of molecular (response) properties is done within a limited orbital space of the solute only, FDE is very efficient, especially in the case of response properties. It has been applied successfully to the calculation of solvatochromic shifts of electronic excitation energies[15,43] and of electron spin resonance hyperfine coupling constants in solution.[44]

Both DRF and FDE are promising approaches for the calculation of molecular (response) properties in solution, mainly because their efficiency allows the calculation of molecular properties for a large number of solvent structures. In addition, both DRF and FDE introduce a "natural partitioning" of the supermolecular system into a solute and a solvent system, which makes it possible to uniquely define molecular properties in solution.

Even though both methods have been applied to the calculation of ground state and response properties in solution in a number of earlier studies, there are several open questions. The DRF model relies on fitted parameters for atomic charges and polarizabilities and it is unclear if this parameterization is generally applicable. In the FDE scheme, an approximate non-additive kinetic energy functional has to be used.[42] Furthermore, in the calculation of response properties the response of the (frozen) solvent is neglected. The approximations that are made in the two methods are quite different and their importance for the calculation of different molecular properties is not fully tested.

In this paper we present a detailed comparison of the DRF model and the FDE scheme for calculating different molecular properties in solution. For this comparison, we use a simple test system, a water molecule inside a solvation shell consisting of 127 water molecules. This system is a well established benchmark for the assessment of discrete solvent models.[7–9,37,45] Since we are only interested in a comparison of the two different solvent models for the calculation of molecular properties, we did not average over a large number of snapshots, but only use one solvent structure instead. This allows us to focus on the differences in the description of the solvent effects.

This work is organized as follows. In section 2, a brief introduction into the theoretical background of FDE and DRF is given. In section 3, we present a detailed comparison of these two solvent models for a water molecule solvated in water. First, in section 3.1, the solvent models are compared for ground state properties, namely the dipole and the quadrupole moment. This is followed by a comparison of the performance of DRF and FDE for response properties. In section 3.2, they are compared for the calculation of electronic excitation energies and in section 3.3 for the calculation of static and frequency-dependent polarizabilities. Concluding remarks follow in section 4.

2. Methodology

2.1. Frozen-density embedding

In the frozen-density embedding (FDE) formalism[41] the electron density of the embedded subsystem (ρ_{I}) in a given microscopic environment, which is represented by means of its electron density (ρ_{II}) and a set of nuclear charges ($Z_{A\mathrm{II}}$) at the corresponding positions ($\boldsymbol{R}_{A\mathrm{II}}$), is derived from KS-like one-electron equations.

The effective potential in these equations can be derived from the requirement that the total density $\rho_{\mathrm{tot}}(\boldsymbol{r}) = \rho_{\mathrm{I}}(\boldsymbol{r}) +$

$\rho_{II}(\boldsymbol{r})$ of the system is obtained in an optimization process in which the electron density $\rho_{II}(\boldsymbol{r})$ of the environment is kept frozen. On the assumption that the complementary $\rho_I(\boldsymbol{r})$ is positive definite and is non-interacting pure-state v_s-representable,[26] we obtain KS-like equations in which the effect of $\rho_{II}(\boldsymbol{r})$ is represented by an embedding term in the effective potential for the $\rho_I(\boldsymbol{r})$ system,[41]

$$\left[-\frac{\nabla^2}{2} + V_{\text{eff}}^{\text{KS}}[\rho_I](\boldsymbol{r}) + V_{\text{eff}}^{\text{emb}}[\rho_I, \rho_{II}](\boldsymbol{r})\right] \phi_i^{(I)}(\boldsymbol{r}) = \varepsilon_i \phi_i^{(I)}(\boldsymbol{r}), \quad i = 1, \ldots, N_I. \tag{1}$$

In these equations, $V_{\text{eff}}^{\text{KS}}[\rho_I](\boldsymbol{r})$ is the KS effective potential of the isolated subsystem I and $V_{\text{eff}}^{\text{emb}}[\rho_I, \rho_{II}](\boldsymbol{r})$ is the embedding potential which reads

$$\begin{aligned} V_{\text{emb}}^{\text{eff}}[\rho_I, \rho_{II}](\boldsymbol{r}) = &\sum_{A_{II}} -\frac{Z_{A_{II}}}{|\boldsymbol{r} - \boldsymbol{R}_{A_{II}}|} + \int \frac{\rho_{II}(\boldsymbol{r}')}{|\boldsymbol{r}' - \boldsymbol{r}|}\, \mathrm{d}\boldsymbol{r}' \\ &+ \left.\frac{\delta E_{\text{xc}}[\rho]}{\delta\rho}\right|_{\rho=\rho_{\text{tot}}} - \left.\frac{\delta E_{\text{xc}}[\rho]}{\delta\rho}\right|_{\rho=\rho_I} \\ &+ \left.\frac{\delta T_s[\rho]}{\delta\rho}\right|_{\rho=\rho_{\text{tot}}} - \left.\frac{\delta T_s[\rho]}{\delta\rho}\right|_{\rho=\rho_I}, \end{aligned} \tag{2}$$

where the exchange–correlation ($E_{\text{xc}}[\rho]$) and kinetic energy ($T_s[\rho]$) functionals are defined in the KS formulation of DFT. The kinetic energy part of the potential is sometimes written as the functional derivative $\delta T_s^{\text{nadd}}[\rho_I, \rho_{II}]/\delta\rho_I$ of the non-additive kinetic energy functional,

$$T_s^{\text{nadd}}[\rho_I, \rho_{II}] = T_s[\rho_I + \rho_{II}] - T_s[\rho_I] - T_s[\rho_{II}] \tag{3}$$

If the initial assumptions are fulfilled, *i.e.*, if $\rho_{\text{tot}}(\boldsymbol{r}) - \rho_{II}(\boldsymbol{r})$, is positive definite and non-interacting pure-state v_s-representable, the solution of eqn (1) will yield the exact ground state electron density.[42] This makes this scheme an exact approach in the exact functional limit, in contrast to most other embedding methods commonly used in practical computer simulations.

However, in practical calculations an approximate non-orbital-dependent functional is used for the non-additive kinetic energy functional and its functional derivative because the KS orbitals of the full system are not known. Based on previous results[46–48] we selected the PW91k kinetic energy functional.[49]

Since eqn (1) can be solved for any postulated electron density, $\rho_{II}(\boldsymbol{r})$ may also be obtained from simpler considerations.[41] For instance, a solvent can be modeled by using just a sum of electron densities of the individual solvent molecules.[15,43,46,50] In this work, we used two different ways of modeling the electron density of the solvent. First, we used a simple sum-of-molecular-fragments approach as introduced in ref. 15. In this approach the solvent density is constructed as a sum of the electron densities of isolated solvent molecules. Since the solvent structure used in this work consists of rigid water molecules, it is even possible to use the same electron density for each solvent molecule.

This approximated electron density of the environment can be improved by including the effects of relaxation of the solvent using "freeze-and-thaw" iterations,[51] *i.e.*, by exchanging the role of the frozen and the non-frozen system. In this work, this is done using the partial relaxation scheme described in ref. 43. For the ten solvent molecules closest to the solute molecule the electron density was updated using two freeze-and-thaw cycles,[51] while for the outer solvent molecules we still use the sum-of-molecular-fragments density as described above. The frozen density of these outer solvent molecules is taken into account during all freeze-and-thaw cycles.

A time-dependent linear response generalization of this embedding scheme was derived in ref. 52. Under the assumption that the response to an external electromagnetic field in resonance with an electronic transition of the embedded molecule is localized to the non-frozen system (system I), *i.e.*, that the response of the frozen environment (system II) can be neglected, this leads—in addition to the kernel within the adiabatic local density approximation (ALDA) in conventional TDDFT—to an effective embedding kernel (see the supplementary material to ref. 53),

$$f_{\text{xc}}^{\text{emb}}(\boldsymbol{r}, \boldsymbol{r}') = \left.\frac{\delta^2 E_{\text{xc}}[\rho]}{\delta\rho(\boldsymbol{r})\delta\rho(\boldsymbol{r}')}\right|_{\rho=\rho_I+\rho_{II}} - \left.\frac{\delta^2 E_{\text{xc}}[\rho]}{\delta\rho(\boldsymbol{r})\delta\rho(\boldsymbol{r}')}\right|_{\rho=\rho_I} + \frac{\delta^2 T_s^{\text{nadd}}[\rho_I, \rho_{II}]}{\delta\rho_I(\boldsymbol{r})\delta\rho_I(\boldsymbol{r}')}, \tag{4}$$

which now also contains a contribution of the non-additive kinetic energy. This contribution is, for consistency with the ALDA-kernel, approximated by using the (local density) Thomas–Fermi functional in eqn (4). This means that the additional term depending on the solvent response function in the exact formulation in ref. 52 is assumed to be negligible, and the exchange–correlation kernel in eqn (4) is evaluated for the density ρ_{II} of the ground state calculation. An alternative interpretation is that an assumption is made which assumes that the whole response can be described in terms of a change in the density ρ_I.

2.2. The discrete reaction field model

The DRF model is a polarizable QM/MM model. The solvent is represented by atomic charges q_s and polarizabilities α_s that are placed at positions $\boldsymbol{R}_s$. Although the DRF model can describe a frequency-dependent atomic polarizability,[54,55] we will assume that the atomic polarizabilities are independent of the frequency. This is expected to be a reasonable assumption due to the small dispersion of the polarizability in the frequency range that lies well below any electronic excitation. In the DRF model the QM/MM operator at a point $\boldsymbol{r}$ is given as an extra term in the effective potential in the KS equations,[8]

$$\left[-\frac{\nabla^2}{2} + V_{\text{eff}}^{\text{KS}}[\rho](\boldsymbol{r}) + V^{\text{DRF}}[\rho](\boldsymbol{r})\right]\phi_i(\boldsymbol{r}) = \varepsilon_i\phi_i(\boldsymbol{r}), \quad i = 1, \ldots, N. \tag{5}$$

where the DRF potential is given by

$$\begin{aligned} V^{\text{DRF}}[\rho](\boldsymbol{r}) &= V^{\text{el}}(\boldsymbol{r}) + V^{\text{pol}}[\rho](\boldsymbol{r}) \\ &= \sum_s \frac{q_s}{|\boldsymbol{r} - \boldsymbol{R}_s|} + \sum_s \boldsymbol{\mu}_s^{\text{ind}} \cdot \frac{(\boldsymbol{r} - \boldsymbol{R}_s)}{|\boldsymbol{r} - \boldsymbol{R}_s|^3}. \end{aligned} \tag{6}$$

The first term, V^{el}, describes the Coulomb interaction between the QM system (the solute) and the permanent charge

distribution of the solvent molecules. The second term, V^{pol}, describes the many-body polarization of the solvent molecules.

The induced atomic dipole at a site s is given by

$$\mu_s^{\mathrm{ind}} = \alpha_s \left[\mathrm{F}_s^{\mathrm{init}} + \sum_{t,t\neq s} \boldsymbol{T}_{st}^{(2)} \boldsymbol{\mu}_t^{\mathrm{ind}} \right], \tag{7}$$

where $\boldsymbol{T}_{st}^{(2)}$ is the screened dipole interaction tensor[8,56,57] for the interaction between sites s and t. The induced dipole arises from the field $\boldsymbol{F}_s^{\mathrm{init}}$ at site s that is due to the electronic charge distribution of the QM part, the field from the QM nuclei, and the field from the point charges at the solvent molecules as well as the field from all other induced dipoles. The induced dipole moments are therefore calculated self-consistently in every iteration of the KS procedure.

The combination of the DRF model with TDDFT linear response theory was presented in ref. 9. It introduces an additional contribution in the TDDFT kernel that describes the change in the DRF potential of eqn (6) due to a perturbation in the electron density of the QM system, *i.e.*, the response of the atomic polarizabilities. This additional contribution is given by

$$\begin{aligned} f^{\mathrm{DRF}}(\boldsymbol{r},\boldsymbol{r}') &= \frac{\delta V^{\mathrm{DRF}}[\rho](\boldsymbol{r})}{\delta\rho(\boldsymbol{r}')} \\ &= \sum_s \sum_t \frac{(\boldsymbol{r}'-\boldsymbol{R}_t)}{|\boldsymbol{r}'-\boldsymbol{R}_t|^3} \cdot \boldsymbol{B}_{st} \frac{(\boldsymbol{R}_s-\boldsymbol{r})}{|\boldsymbol{R}_s-\boldsymbol{r}|^3}. \end{aligned} \tag{8}$$

In this equation $\boldsymbol{B}_{st}$ is the relay matrix that relates the induced dipole moment at site s to the electric field at site t and that is defined by

$$\boldsymbol{\mu}_s^{\mathrm{ind}} = \sum_t \boldsymbol{B}_{st} \boldsymbol{F}_t. \tag{9}$$

This relay matrix is never calculated explicitly, but the induced dipole moments due to the first-order change in the electron density are calculated iteratively by solving eqn (7) in the linear response calculation. Details can be found in ref. 9.

2.3. Computational details

All density functional calculations were performed using the Amsterdam Density Functional (ADF) package.[58,59] The "statistical averaging of molecular orbital potentials" (SAOP) potential[60–62] was used to approximate the exchange–correlation potential, since it is well suited for the calculation of response properties. To provide a consistent comparison we also employed the SAOP potential for ground state properties, even though it has been found that SAOP is less reliable in this case.[63]

All calculations were done using the VDiff basis set from the ADF basis set library, which is a triple-ζ-quality Slater basis set containing additional diffuse functions. Previous studies[8,9] showed that this basis set is sufficiently large for the accurate calculation of both the ground state and response properties investigated here. This was confirmed in the present work by test calculations using the large even-tempered ET-QZ3P-3DIFFUSE Slater basis set, in which the results did not change significantly.

In the FDE calculations, the initial solvent density was constructed as a sum of the electron densities of molecular fragment calculated using the local-density approximation (LDA) and a DZP basis set. In the FDE calculations using the orbital-dependent SAOP potential, the exchange–correlation component of the effective embedding potential was approximated using the Becke–Perdew–Wang (BPW91) exchange–correlation functional.[64,65]

The parameters needed for the solvent molecules in the DRF model, *i.e.*, point charges and atomic polarizabilities, were adopted from ref. 8. The point charges are $q_H = 0.3345$ a.u. and $q_o = -0.6690$ a.u. which generate a molecular dipole moment of 1.88 Debye. The atomic polarizabilities are $\alpha_H = 0.0690$ a.u. and $\alpha_o = 9.3005$ a.u. which reproduced the molecular polarizability tensor with a mean polarizability of 9.62 a.u. and a polarizability anisotropy of 0.52 a.u. The screening parameter, $a = 2.1304$, used in eqn (7), was taken from ref. 57.

The calculations of excitation energies and polarizabilities were done using the TDDFT implementation of ADF.[66,67] The finite field calculations of the polarizabilities in section 3.3 were performed using an electric field of 0.001 a.u. To obtain the static mean polarizability, six separate calculations were performed in which an electric field was applied in the x, y, and z direction. The individual components of the polarizability tensor were then obtained by numerical differentiation of the dipole moment.

3. Results and discussion

The comparison of the DRF and FDE solvent models is carried out for the system investigated in ref. 8 and 9, where a water molecule in the "liquid phase" was studied. It is a fixed structure of 128 rigid water molecules. The structure was obtained from a molecular dynamics simulation using a polarizable force field in an earlier work.[45] One of the 128 water molecules is considered as the solute, while the remaining 127 form the solvent shell. The structure of the water molecule inside the solvent shell is shown in Fig. 1 and the coordinates are given in the electronic supplementary material (ESI).†

We note that by using only one solvent structure any effects of the dynamics of the solvent are neglected, *i.e.*, the fluctuations in the geometrical structure of both the solute and the solvent molecules are not taken into account and replaced by a static picture. For correctly describing all solvent effects it would be necessary to include a large number of solvent structures instead of just one average configuration.[15,43] It will therefore be difficult to directly compare the obtained results to experimental values. However, the error that results from neglecting the dynamical effects will be made consistently in all calculations. As the purpose of this study is to provide a comparison of different solvent models, this consistent error is not relevant for the conclusions drawn here. Furthermore, the restriction to only one structure enables us to do a very detailed analysis of the results and greatly simplifies their interpretation.

3.1. Dipole and quadrupole moments

First, we compare the performance of DRF and FDE for dipole and quadrupole moments. These are both ground state

Fig. 1 Structure of a water molecule inside a solvent shell of 127 water molecules. The "solvated" water molecule is the one that is highlighted, the other water molecules are considered to belong to the solvent shell. Coordinates are given in the ESI.†

properties that depend directly on the electron density. They are a sensitive measure for the distribution of the electron density obtained within the different solvent models. Table 1 gives the dipole and quadrupole moments that were calculated for the isolated water molecule and for the water molecule in the "liquid phase", *i.e.*, inside the solvation shell of 127 water molecules.

For the isolated molecule, the calculated dipole moment overestimates the experimental value[68] of 1.854 D. This overestimation is a artifact of the use of the SAOP exchange–correlation potential that was primarily developed to yield accurate response properties. For the water molecule in solution, DRF predicts a shift in the dipole moment of 0.73 D. This increase in the dipole moment of water in the liquid phase relative to the gas phase has been discussed in detail in ref. 8. The obtained values agree with previous CCSD calculations[45] using a solvent model similar to DRF and were also found to be within suggested limits that can be deduced from experiment.[8]

The FDE calculations using a sum-of-molecular-fragments electron density for the solvent [labeled FDE(SumFrag)] predict a shift in the dipole moment that is significantly smaller than that predicted by DRF. The situation changes when relaxation of the solvent electron density is included in the FDE calculations [labeled FDE(relaxed)]. In this case, the calculated dipole moments are in good agreement with the dipole moment calculated using DRF. This shows that the effect of polarization of the solvent density is of great importance for the correct description of the dipole moment in the system considered here. It was already noticed in earlier works[43,53] that the inclusion of relaxation has a strong influence in systems with direct hydrogen bonds between the solvated molecule and the solvent. Since relaxation is needed mainly for the correct description of hydrogen bonds it is sufficient to relax the solvent molecules that are close to the solvated molecule whereas relaxation of the outer solvent shells can safely be neglected.[43]

In FDE the effect of relaxation of the solvent density, *i.e.*, of changes in the solvent electron density due to the solvated molecule, has to be included explicitly using freeze-and-thaw cycles. In DRF calculations a discrete model of the same effect is used, where the polarization of the solvent electron density is modeled using distributed atomic polarizabilities that can be obtained from gas phase calculations. While this strategy of modeling the change of the solvent density is computationally more efficient than the full treatment in FDE, the FDE description should be more accurate, especially at short distances where the discretization of the charge distribution gives larger errors.

For the quadrupole moments, the shift from the gas to the liquid phase is smaller than for the dipole moment. The quadrupole moments calculated using DRF and FDE are in good agreement. While the effect of relaxation in the FDE calculations is large for the dipole moment, this is not the case for the quadrupole moment.

Summarizing these results, we find that for the dipole and quadrupole moments DRF and FDE give results that are very similar if relaxation of the innermost solvent molecules is included in FDE. Since both the dipole and the quadrupole moment only depend on the calculated electron density, these results give a good indication that the electron densities calculated within the different solvent models are not very different.

Table 1 Dipole moments $\boldsymbol{\mu}$, solvation shifts in dipole moments $\Delta^{\mathrm{solv}}\mu$ relative to the isolated molecule, and traceless quadrupole moments $\boldsymbol{Q}$ for an isolated water molecule in the gas phase and inside a solvation shell of 127 water molecules modeled using DRF as well as FDE. For FDE results are given with an unrelaxed sum-of-molecular-fragments electron density for the solvent (SumFrag) and with a solvent density in which the density of the ten innermost water molecules is relaxed with respect to the solute (relaxed)

	μ/D	$\Delta^{\mathrm{solv}}\boldsymbol{\mu}$/D	$\boldsymbol{Q}_{xx}$/a.u.	$\boldsymbol{Q}_{yy}$/a.u.	$\boldsymbol{Q}_{zz}$/a.u.
Isolated	1.80		1.79	–1.86	0.07
DRF	2.66	+0.86	2.05	–2.15	0.11
FDE (SumFrag)	2.45	+0.65	2.04	–2.12	0.09
FDE (relaxed)	2.71	+0.91	2.09	–2.17	0.08

3.2. Excitation energies

After comparing DRF and FDE for ground state properties, we investigate the performance of the different solvent models for properties depending on the density response, starting with the electronic excitation energies. Table 2 gives the excitation energies of the three lowest excitations of an isolated water molecule and of the corresponding excitations for the system described in the previous section, a water molecule inside a solvation shell consisting of 127 water molecules. Additionally, the solvation shifts of the excitation energies and the oscillator strengths of the corresponding transitions are reported.

The excitation spectra of water in the gas and condensed phase are known experimentally[69–71] and have been discussed in detail before (see, *e.g.*, ref. 72). The gas phase spectrum shows two very diffuse bands with absorption maxima at 7.4 and 9.7 eV, which are assigned to the $1^1A_1 \rightarrow 1^1B_1$ and to the $1^1A_1 \rightarrow 2^1A_1$ transition, respectively. Qualitatively, both excitations have significant Rydberg character. The $1^1A_1 \rightarrow 1^1A_2$

Table 2 Excitation energies E_{ex} of the three lowest excitations for an isolated water molecule in the gas phase and of the corresponding excitations for a water molecule inside a solvation shell of 127 water molecules modeled using DRF and FDE. The solvation shifts of the excitation energies $\Delta^{solv}E_{ex}$ and the oscillator strength f are also given

	$1^1A_1 \rightarrow 1^1B_1$			$1^1A_1 \rightarrow 1^1A_2$			$1^1A_1 \rightarrow 2^1A_1$		
	E_{ex}/eV	$\Delta^{solv}E_{ex}$/eV	f/a.u.	E_{ex}/eV	$\Delta^{solv}E_{ex}$/eV	f/a.u.	E_{ex}/eV	$\Delta^{solv}E_{ex}$/eV	f/a.u.
Isolated	7.76		0.05	9.61		0.00	9.72		0.09
DRF	8.41	+0.65	0.08	10.38	+0.77	0.011	10.40	+0.68	0.11
FDE (SumFrag)	8.71	+0.95	0.07	10.43	+0.82	0.0023	10.70	+0.98	0.04
FDE (relaxed)	8.88	+1.12	0.07	10.69	+1.08	0.0011	11.01	+1.29	0.06

transition, which is the second excitation in the calculations, is dipole forbidden in the gas phase. The excitation spectrum of liquid water shows two very broad overlapping bands. The first band has a maximum at 8.2 eV (corresponding to a solvent shift of approximately 0.8 eV), while the maximum of the second band is at 9.9 eV (corresponding to a much smaller solvent shift of 0.2 eV).

The Rydberg character of the excitations requires the use of a large number of diffuse functions in the basis set and of an asymptotically correct exchange–correlation potential like SAOP.[73,74] If this is taken care of, the results for the isolated molecule in the gas phase are in good agreement with the experimental values. For the water molecule in the "liquid phase", DRF predicts solvent shifts of approximately 0.7 eV for the three lowest transitions. These results have already been discussed in ref. 9. The predicted solvent shifts are of similar size for the first and third excitation. For the first excitation, the calculated solvent shift is in fair agreement with experiment, but there is a significant overestimation of the solvent shift for the third excitation.

FDE using a sum-of-molecular-fragments solvent density predicts significantly larger solvent shifts than DRF. The shifts increase even further to roughly 1.2 eV if relaxation of the solvent density is included. In this case, FDE predicts solvent shifts that are larger than the shifts predicted by DRF by 0.47, 0.31, and 0.61 eV for the first, second, and third transition, respectively. Like DRF, FDE also predicts similar solvent shifts for the first and third transition. The shifts predicted by FDE are larger than those obtained with DRF, but for the lowest excitation there is still a fair agreement with the experimentally observed shift. However, FDE does not describe the lower solvent shift for the third transition correctly. As mentioned earlier, it is difficult to directly compare the obtained solvent shifts to experiment, because we only considered one average solvent structure.

The accuracy of the two different solvent models for the electronic excitations investigated here can be assessed by a comparison to the results of a supermolecular DFT calculation. Such a supermolecular calculation contains all interactions that are modeled in DRF and FDE explicitly, so that it can provide information about the quality of the approximations made in the two models. Obtaining the excitation energies of interest from a supermolecular calculation is problematic, because the charge transfer excitation problem in TDDFT leads to a large number of artificially too low excitations in the energy range of interest.[15] In addition, for the system investigated here, where the solvent is also water, the lowest excitation energies of the solvent molecules will also perturb the analysis.

To minimize these problems, the comparison with a supermolecular calculation is done for a small cluster consisting only of the water molecule in question and of the two closest solvent water molecules. The structure is a substructure of the larger cluster containing 127 solvent molecules and is shown in Fig. 2. In this structure, the "solvated" water molecule is involved in two hydrogen bonds.

Even though in this small cluster the solvent shift of the excitation energies will be much smaller than for the larger water cluster considered earlier, the main cause of the differences between DRF and FDE is expected to originate from the innermost solvent molecules. This small cluster will therefore already provide useful information.

The excitation energies of the lowest excitation energy of the "solvated" water molecule calculated using DRF and FDE as well as a supermolecular calculation are given in Table 3. In the supermolecular calculation, the DZP basis set was used for the two solvent molecules for consistency with the FDE calculation. As in all previous calculations, the VDiff basis set is used for the solute molecule. The transition corresponding to the lowest excitation of the isolated water molecule is identified using the transition density overlap criterion introduced in ref. 15. The excitation found to have the largest overlap with the lowest transition of the isolated water molecule is the seventh excitation in the supermolecular calculation.

The solvent shift obtained using FDE is in reasonable agreement with the result of the supermolecular calculation, with FDE slightly underestimating the supermolecular result by 0.13 eV. In contrast to this, DRF yields a value that significantly underestimates the solvent shift by 0.35 eV. This

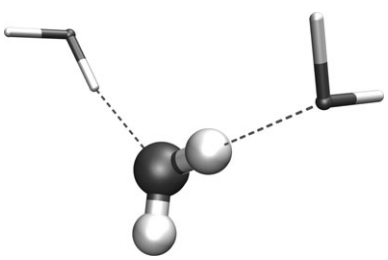

Fig. 2 Structure of the cluster containing a water molecule and the two closest solvent water molecules. The "solvated" water molecule is the one that is highlighted, the other two water molecules are considered to belong to the solvent shell.

Table 3 Excitation energies E_{ex} and solvation shifts in excitation energies $\Delta^{solv}E_{ex}$ of the lowest excitation of a water molecule in the gas phase and in a cluster with two solvent water molecules, modeled using DRF and FDE. In addition, the results of a supermolecular KS-DFT calculation of the same cluster are given, see text for details

	E_{ex}/eV	$\Delta^{solv}E_{ex}$/eV
Isolated	7.76	
DRF	8.08	+0.32
FDE (relaxed)	8.30	+0.54
Supermolecule	8.43	+0.67

indicates that for the calculation of excitation energies the FDE scheme provides an approximation that is closer to the full description of the solvent effects than the DRF model. In the following we will analyze the reasons for the differences in the excitation energies obtained with DRF and FDE and try to identify the problems and shortcomings of the different solvent models. For this analysis we will focus on the lowest excitation only.

For this analysis we split up the calculated excitation energies into different components,

$$E_{ex} = \Delta\varepsilon + \Delta^{resp}_{vac}E_{ex} + \Delta^{resp}_{env}E_{ex}. \quad (10)$$

In this equation, $\Delta\varepsilon$ is the orbital energy difference, *i.e.*, for the excitation studied here the difference between the orbital energies of the highest occupied molecular orbital (HOMO) and the lowest unoccupied molecular orbital (LUMO). The ''vacuum'' response contribution $\Delta^{resp}_{vac}E_{ex}$ is the correction that TDDFT applies to the HOMO–LUMO gap if the effects of the environment are only included in the KS step but not in the TDDFT part of the calculation. It is calculated by subtracting the HOMO–LUMO gap, obtained for the solvated water molecule, from the excitation energy that is calculated from the embedded orbitals without including any additional contributions of the solvent model in the exchange–correlation kernel. It is important to note that for the calculations using solvent models, both the HOMO–LUMO gap $\Delta\varepsilon$ as well as the ''vacuum'' contribution $\Delta^{resp}_{vac}E_{ex}$ include the effect of the solvent model on the ground state orbitals and orbital energies.

In addition to this effect on the ground state orbitals, both solvent models employed here introduce an additional term in the exchange–correlation kernel that gives rise to the environment contribution $\Delta^{resp}_{env}E_{ex}$. For DRF, this additional contribution is given by eqn (8) and describes the response of the induced dipoles on the solvent to the change in electronic density upon excitation. For FDE, the additional contribution is given by the effective embedding kernel of eqn (4) that arises from the contribution of the non-additive kinetic energy and the non-additivity of the exchange–correlation functional and its derivatives.

The results of the decomposition of the excitation energies according to eqn (10) for the isolated and solvated water molecules described using either DRF or FDE are given in Table 4. The differences in the calculated excitation energies are mainly explained by the effects that the solvent models have on the HOMO–LUMO gap, which amounts to 0.70 eV for DRF and 1.08 eV for FDE. The ''vacuum'' response

Table 4 Analysis of the excitation energies calculated for an isolated water molecule and for a water molecule inside a solvent shell of 127 water molecules using DRF and FDE to model the solvent shell. The HOMO–LUMO gap $\Delta\varepsilon$ calculated for the ground state is given as a first order approximation to the excitation energy. The term $\Delta^{resp}_{vac}E_{ex}$ refers to the correction to this gap as calculated using TDDFT without including any contributions of the environment. The additional contributions of the environment to the excitation energies are given as $\Delta^{resp}_{env}E_{ex}$

	$\Delta\varepsilon$/eV	$\Delta^{resp}_{vac}E_{ex}$/eV	$\Delta^{resp}_{env}E_{ex}$/eV	E_{ex}/eV
Isolated	7.59	+0.17	—	7.76
DRF	8.29	+0.15	−0.03	8.41
FDE (relaxed)	8.67	+0.14	+0.07	8.88

correction $\Delta^{resp}_{vac}E_{ex}$ is of similar size for both the isolated molecule calculation and the calculations in solution (DRF and FDE). The difference is only approximately −0.03 eV, which is negligible compared to the large change in the HOMO–LUMO gap that is induced by the solvation shell.

The additional environment correction $\Delta^{resp}_{env}E_{ex}$ is also small compared to the change in the HOMO–LUMO gap caused by the solvation shell. However, these corrections are responsible for part of the differences that are observed between DRF and FDE. In DRF the environment correction is negative, *i.e.*, it lowers the calculated excitation energy, because the response of the solvent stabilizes the excited state. In FDE, the environment contribution is positive and therefore increases the excitation energy. This is because the effective embedding kernel in FDE contains the effects of the Pauli repulsion of the solvent molecules, which will destabilize the excited state. These environmental contributions in DRF and FDE are largely complementary, *i.e.*, each of them is describing an effect that is missing in the other model. In total, the different description of the solvent effects in TDDFT causes a difference in the excitation energies of 0.10 eV. This is a small part of the total difference between DRF and FDE of 0.47 eV.

The differences in the HOMO–LUMO gap are mainly caused by two effects that are included in FDE but are absent in the DRF model. First, the effects of hydrogen bonding are only partly included in the purely electrostatic DRF model. For the solvated water molecule considered here, the HOMO is stabilized by hydrogen bonding, while the LUMO is destabilized. Hydrogen bonding thus leads to an increase in the HOMO–LUMO gap. This chemical bonding part of the hydrogen bonding should be described correctly by FDE, while DRF only contains the electrostatic part. As a second effect, FDE also includes the Pauli repulsion of the solvent. The unoccupied orbitals partly extend into regions that are occupied by solvent molecules and experience the Pauli repulsion of their electrons. This leads to a further increase in the orbital energies of the diffuse unoccupied orbitals and therefore to an increase in the HOMO–LUMO gap. This is especially important in the system investigated here, since the lowest excitation is quite diffuse.

3.3. Polarizabilities

Finally, we compare the performance of DRF and FDE for modeling solvent effects on polarizabilities, again using the

same solvent structure. In Table 5, for both the isolated molecule and the water molecule in the solvent cage the calculated mean polarizabilities and the polarizability anisotropies γ are given. Both the static polarizabilities and the frequency-dependent polarizabilities at the frequencies ω = 0.0428, 0.0570, 0.0856 a.u. (λ = 1064, 800, 532 nm, respectively) are given.

The static mean polarizability of 9.40 a.u. calculated for the isolated molecule is in good agreement with both the results of previous CCSD(T) calculations[75] (9.62 a.u.) and with the experimental value of 9.83 a.u. taken from ref. 76. For the frequency-dependent polarizabilities our DFT results are in good agreement with previous CCSD calculations[37] that obtained mean polarizabilities of 9.52, 9.57, and 9.71 a.u. calculated at frequencies of 0.0428, 0.0570, and 0.0856 a.u., respectively.

For the water molecule inside the solvation shell of 127 water molecules, DRF predicts a slight increase in the mean polarizability of approximately 0.2 a.u., both for the static and frequency-dependent polarizabilities. For the polarizability anisotropy, DRF predicts a slight decrease, in agreement with the previous results of ref. 9. With FDE, the mean polarizability decreases in solution by approximately 0.7 a.u. compared to the isolated molecule, which is in contrast to the increase in polarizability that was found with DRF. The polarizability anisotropies calculated using FDE are in qualitative agreement with the DRF calculations, but FDE predicts a lowering about twice as large as predicted by DRF. We further note that for the calculation of the polarizabilities the relaxation of the solvent density in the FDE approach is much less important than for dipole moments and excitation energies.

The most striking finding of this comparison is the qualitative difference between DRF and FDE for the mean polarizabilities. With DRF the mean polarizability increases in solution, whereas it decreases with FDE. To analyze the qualitative differences between DRF and FDE, we performed an analysis similar to that in section 3.2 for the excitation energies. We decomposed the calculated shifts of the mean polarizability in solution into contributions due to changes in the (ground state) molecular orbitals and solvent contributions in the linear response calculation. To simplify this analysis, we focus on the static mean polarizabilities.

Table 5 Static and frequency-dependent polarizabilities calculated for an isolated water molecule in the gas phase and inside a solvation shell of 127 water molecules modeled using DRF and FDE. The mean polarizabilities $\bar{\alpha}$ and the polarizability anisotropy γ are given

	ω/a.u.	$\bar{\alpha}$/a.u.	γ/a.u.
Isolated	0.0000	9.40	0.91
	0.0428	9.47	0.89
	0.0570	9.51	0.88
	0.0856	9.65	0.82
DRF	0.0000	9.62	0.72
	0.0428	9.68	0.71
	0.0570	9.73	0.71
	0.0856	9.87	0.70
FDE (SumFrag)	0.0000	8.77	0.47
	0.0428	8.82	0.47
	0.0570	8.86	0.46
	0.0856	8.98	0.46
FDE (relaxed)	0.0000	8.67	0.50
	0.0428	8.72	0.50
	0.0570	8.76	0.50
	0.0856	8.87	0.50

Table 6 Analysis of the static mean polarizabilities calculated for an isolated water molecule and for a water molecule inside a solvent shell of 127 water molecules using DRF and FDE to model the solvent shell. The mean polarizability calculated without including any effects of the environment in the TDDFT calculation is given as $\bar{\alpha}_{\mathrm{noenv}}$. The additional contributions of the environment to the polarizabilities are given as $\Delta_{\mathrm{env}}^{\mathrm{resp}}\alpha$. The resulting mean polarizability is given as $\bar{\alpha}_{\mathrm{tot}}$

	$\bar{\alpha}_{\mathrm{noenv}}$/a.u.	$\Delta_{\mathrm{env}}^{\mathrm{resp}}\alpha$/a.u.	$\bar{\alpha}_{\mathrm{tot}}$/a.u.
Isolated	9.40	—	9.40
DRF	9.22	+0.40	9.62
FDE (relaxed)	8.78	−0.11	8.67

The static mean polarizabilities calculated using the different solvent models are decomposed according to

$$\bar{\alpha}_{\mathrm{tot}} = \bar{\alpha}_{\mathrm{noenv}} + \Delta_{\mathrm{env}}^{\mathrm{resp}}\alpha, \qquad (11)$$

where $\bar{\alpha}_{\mathrm{noenv}}$ is the static mean polarizability calculated from the embedded orbitals without including the additional environmental contributions in the linear response calculation. The results of this analysis are given in Table 6.

The mean polarizabilities $\bar{\alpha}_{\mathrm{noenv}}$ follow the trend that is given by the solvent shifts of the excitation energies, since larger excitation energies should qualitatively correspond to a smaller mean polarizabilities. In the case of a larger solvent shift of the excitation energies, the mean polarizability without the environment contribution decreases. For DRF, the mean polarizability in solution decreases by 0.18 a.u. compared to the isolated molecule, which is in agreement with the larger excitation energies. For FDE, where the solvent shift of the excitation energies is even larger than in DRF, the mean polarizability in solution decreases by 0.62 a.u. compared to the isolated molecule.

The qualitative differences between DRF and FDE are caused by the environmental corrections to the mean polarizabilities $\Delta_{\mathrm{env}}^{\mathrm{resp}}\alpha$ that appear when the contributions of the environment are also included in the TDDFT part of the calculation. In the case of the DRF calculation, this correction contains the effect of the response of the solvent to the polarization of the solvated molecule. This response stabilizes the polarized molecule and therefore leads to an increase in the polarizability. This correction to the mean polarizability of +0.40 a.u. is larger than the change in the polarizability due to the changed molecular orbitals in solution of −0.18 a.u. and leads to an overall increase in the mean polarizability in solution. For the FDE calculation, where the response of the solvent is neglected, the environmental correction is much smaller than the corresponding DRF correction and is of opposite sign, *i.e.*, the environment destabilizes the polarized molecule and thus leads to a lower polarizability. Therefore, the FDE correction does not change the lowering of the mean polarizability in solution, which could be estimated from the increase in the excitation energies.

This analysis shows that for the calculation of polarizabilities the inclusion of the solvent response is apparently very

important. For the system considered here, it changes the sign of the solvent effect on the static mean polarizability in the DRF calculation. On the other hand, even though the response of the solvent is included, the ground state orbital energies obtained from DRF are worse than the ones obtained from FDE, because the effects of hydrogen bonding and Pauli repulsion are only partly accounted for.

In the FDE calculation, where the response of the solvent is missing in the current TDDFT extension, it is possible to include the response of the solvent in the FDE calculations by calculating the static polarizabilities from the change in the dipole moment due to a finite electric field. In these calculations one can allow the solvent density to adapt to the polarization of the solute water molecule due to an applied electric field so that the response of the solvent is included. To estimate the effect of the environmental response in the FDE case, we calculate the difference between the static mean polarizabilities obtained from two different series of finite field calculations. In the first calculations, the solvent density is relaxed with respect to the non-polarized solute molecule, whereas it was relaxed with respect to the solute molecule polarized by the applied electric field in the second series of calculations to include the response of the solvent.

The first calculations were performed by converging the electron densities of the solvent and solute in two freeze-and-thaw FDE iterations. As in all earlier calculations, in these freeze-and-thaw iterations only the ten solvent molecules that are closest to the solute are allowed to relax, while for all other solvent molecules the frozen gas phase density is used. The relaxed solvent density was then used as the frozen density in an FDE calculation of the solute water molecule. From the numerical differentiation of the dipole moment obtained in this calculation with respect to the applied electric field, the polarizability tensor was obtained. These calculations yield a static mean polarizability of 7.79 a.u. In these finite field calculations the solvent density cannot respond to the polarization of the solute. The corresponding TDDFT calculation, labeled FDE(relaxed) in Table 5, resulted in a mean polarizability of 8.67 a.u. The difference between these values arise because in the TDDFT calculations the ALDA approximation is used for the exchange–correlation kernel in combination with the SAOP potential. Therefore, the polarizabilities obtained from finite field SAOP calculations do not agree with the TDDFT results. However, since the SAOP potential was designed to be used together with the ALDA kernel, the TDDFT calculations using ALDA should be more accurate than the finite field calculation (which corresponds to a TDDFT calculation using the ''true'' SAOP kernel).[60]

To obtain the polarizability from finite field FDE calculations that take the response of the solvent into account, the electron densities of the solute and solvent were calculated from freeze-and-thaw FDE calculations in which a finite electric field was applied in the calculation of the solute water molecule. The finite electric field was not applied in the calculations of the solvent electron density since we are only interested in the calculation of the local solute polarizability. Including the finite electric field in the solvent calculations would introduce a screening of the macroscopic field at the solute molecule, leading to the so-called effective polarizability.[38] By applying the finite electric field in all calculations of the solute during the freeze-and-thaw cycles, the converged solvent density is relaxed with respect to the polarized solute molecule. The polarizabilities obtained from numerical differentiation of the dipole moments thus include the response of the solvent with respect to the solute polarization. From these calculations, a static mean polarizability of 8.09 a.u. is obtained. The difference between these two sets of finite field FDE calculations, which is our estimate for the effect of the solvent response on the mean polarizability, amounts to +0.30 a.u. This is comparable to the solvent response correction of +0.40 a.u. in the DRF case.

Adding this correction to the static mean polarizability from the TDDFT calculations using FDE to model the solvent leads to an estimated total static mean polarizability of 8.97 a.u., *i.e.*, even when the (positive) correction due to the response of the solvent is taken into account, the FDE calculations still predict a decrease in the static mean polarizability in solution compared to the isolated molecule. The DRF model predicts an increase, because the response of the solvent—modeled by atomic polarizabilities—is the largest solvent effect. In contrast to this, the major solvent effect in the FDE calculation arises from the increased HOMO–LUMO gap and thus leads to a smaller mean polarizability.

4. Conclusions

In this work we performed a detailed comparison of the two discrete solvent models DRF and FDE for a number of molecular properties. For the dipole and quadrupole moment as ground state properties both solvent models lead to similar results. To be able to account for the polarization of the solvent in FDE, it is necessary to relax the solvent density with respect to the solute in freeze-and-thaw cycles. The same effect is included in DRF in a computationally more efficient, though more approximate way by using distributed atomic polarizabilities.

For response properties, there are significant differences between the two solvent models. In the case of the excitation energies of the water system studied here, FDE predicts a larger solvent shift than the DRF model. Our analysis showed that this difference mainly originates from a different description of the ground state molecular orbitals of the solute molecule. The embedded orbitals obtained from the FDE calculation show a larger HOMO–LUMO gap than those obtained in the DRF calculation.

We attribute this difference in the HOMO–LUMO gap to a different description of short-range effects, the most important effects being direct hydrogen bonding between the solute and the solvent as well as the additional Pauli repulsion of the solvent on the diffuse excited states. Since the FDE scheme is in principle exact, it should be able to describe these effects more accurately than the DRF model, where both effects can only be modeled by the parameterization of the atomic point charges and polarizabilities. This was confirmed by a comparison to a supermolecular calculation on a smaller system that agreed well with the excitation energy calculated using FDE, while DRF yields an excitation energy that is too low. The small contribution of the response of the solvent to the

excitation energies shows that the approximation of a response localized on the solute in the FDE calculation of excitation energies is obviously fulfilled.

For the polarizabilities, the effect of the response of the solvent to the polarization of the solute becomes nearly as important as the effect of the solvent on the ground state orbitals, whereas it was negligible for the calculation of excitation energies. The solvent response is modeled in DRF by means of distributed atomic polarizabilities, but it is missing in the TDDFT extension of the FDE scheme. Since it apparently can not be neglected for the calculation of molecular polarizabilities in solution, DRF performs better for this kind of response properties. It can be expected that the effect of the solvent response will become even more important when going to hyperpolarizabilities and other nonlinear optical properties.

The inclusion of the environmental response in DRF does not overcome the problems that are caused by the inaccurate description of the ground state orbitals of the solute. The finite field calculations that were done to get an estimate of the polarizability calculated using FDE including the response of the environment still yield a static mean polarizability that significantly differs from the results of the DRF calculation. In particular, the two models predict a different sign of the solvent shift in the mean polarizability. It would, therefore, be interesting to extend the FDE scheme to explicitly include the response of the solvent, since the finite field approach employed here can only be applied for static polarizabilities. This would make the FDE scheme more generally applicable, *e.g.*, to the calculation of other nonlinear optical properties in solution.

Acknowledgements

The authors acknowledge computer time provided by the Dutch National Computing Facilities (NCF). C.R.J. and L.V. thank The Netherlands Organization for Scientific Research (NWO) for financial support via the TOP program. J.N. gratefully acknowledges funding by a Forschungsstipendium of the Deutsche Forschungsgemeinschaft (DFG).

References

1 C. J. Cramer and D. G. Truhlar, *Chem. Rev.*, 1999, **99**, 2161–2200.
2 J. Tomasi, B. Mennucci and R. Cammi, *Chem. Rev.*, 2005, **105**, 2999–3094.
3 C. J. Cramer, *Essentials of Computational Chemistry*, Wiley, New York, 2002.
4 M. Orozco and F. J. Luque, *Chem. Rev.*, 2000, **100**, 4187–4226.
5 J. Tomasi, *Theor. Chem. Acc.*, 2004, **112**, 184–203.
6 J. Tomasi, R. Cammi, B. Mennucci, C. Cappelli and S. Corni, *Phys. Chem. Chem. Phys.*, 2002, **4**, 5697–5712.
7 T. D. Poulsen, P. R. Ogilby and K. V. Mikkelsen, *J. Chem. Phys.*, 2002, **116**, 3730–3738.
8 L. Jensen, P. Th. van Duijnen and J. G. Snijders, *J. Chem. Phys.*, 2003, **118**, 514–521.
9 L. Jensen, P. Th. van Duijnen and J. G. Snijders, *J. Chem. Phys.*, 2003, **119**, 3800–3809.
10 J. Zeng, N. S. Hush and J. R. Reimers, *J. Chem. Phys.*, 1993, **99**, 1508–1521.
11 K. Coutinho, S. Canuto and M. C. Zerner, *Int. J. Quantum Chem.*, 1997, **65**, 885–891.
12 T. Malaspina, K. Coutinho and S. Canuto, *J. Chem. Phys.*, 2002, **117**, 1692–1699.
13 N. A. Besley, M. T. Oakley, A. J. Cowan and J. D. Hirst, *J. Am. Chem. Soc.*, 2004, **126**, 13502–13511.
14 U. F. Röhrig, I. Frank, J. Hutter, A. Laio, J. VandeVondele and U. Rothlisberger, *ChemPhysChem*, 2003, **4**, 1177–1182.
15 J. Neugebauer, M. J. Louwerse, E. J. Baerends and T. A. Wesolowski, *J. Chem. Phys.*, 2005, **122**, 094115.
16 Y. Luo, P. Norman and H. Ågren, *J. Chem. Phys.*, 1998, **109**, 3589–3595.
17 P. Macak, P. Norman, Y. Luo and H. Ågren, *J. Chem. Phys.*, 2000, **112**, 1868–1875.
18 D. Jonsson, P. Norman, H. Ågren, Y. Luo, K. O. Sylvester-Hvid and K. V. Mikkelsen, *J. Chem. Phys.*, 1998, **109**, 6351–6357.
19 K. V. Mikkelsen, P. Jørgensen, K. Ruud and T. Helgaker, *J. Chem. Phys.*, 1997, **106**, 1170–1180.
20 P.-O. Åstrand, K. V. Mikkelsen, P. Jørgensen, K. Ruud and T. Helgaker, *J. Chem. Phys.*, 1998, **108**, 2528–2537.
21 C.-G. Zhan and D. M. Chipman, *J. Chem. Phys.*, 1999, **110**, 1611–1622.
22 J. Tomasi and M. Persico, *Chem. Rev.*, 1994, **94**, 2027–2094.
23 D. Frenkel and B. Smit, *Understanding Molecular Simulation*, Academic Press, New York, 2nd edn, 2002.
24 R. Car and M. Parrinello, *Phys. Rev. Lett.*, 1985, **55**, 2471–2474.
25 D. Marx and J. Hutter, in *Modern Methods and Algorithms of Quantum Computing, vol. 1 of NIC Series*, ed. J. Grotendorst, John von Neumann Institute for Computing, Jülich, 2000, pp. 257–277.
26 R. G. Parr and W. Yang, *Density-Functional Theory of Atoms and Molecules*, Oxford University Press, Oxford, 1989.
27 E. Runge and E. K. U. Gross, *Phys. Rev. Lett.*, 1984, **52**, 997–1000.
28 M. E. Casida, in *Recent Advances in Density-Functional Methods*, ed. D. P. Chong, World Scientific, Singapore, 1995, pp. 155–192.
29 E. R. Batista, S. S. Xantheas and H. Jónsson, *J. Chem. Phys.*, 1999, **111**, 6011–6015.
30 A. Warshel and M. Levitt, *J. Mol. Biol.*, 1976, **103**, 227–249.
31 B. T. Thole and P. Th. van Duijnen, *Theor. Chim. Acta*, 1980, **55**, 307–318.
32 M. J. Field, P. A. Bash and M. Karplus, *J. Comput. Chem.*, 1990, **11**, 700–733.
33 J. Gao, in *Reviews in Computational Chemistry*, ed. K. B. Lipkowitz and D. B. Boyd, VCH, New York, 1995, vol. 7, pp. 119–185.
34 P. Sherwood, in *Modern Methods and Algorithms of Quantum Computing, Vol. 1 of NIC Series*, ed. J. Grotendorst, John von Neumann Institute for Computing, Jülich, 2000, pp. 257–277.
35 A. Genest, A. Woiterski, S. Krüger, A. M. Shor and N. Rösch, *J. Chem. Theory Comput.*, 2006, **2**, 47–58.
36 J. Kongsted, A. Osted, K. V. Mikkelsen and O. Christiansen, *J. Mol. Struct. (THEOCHEM)*, 2003, **632**, 207–225.
37 J. Kongsted, A. Osted, K. V. Mikkelsen and O. Christiansen, *J. Chem. Phys.*, 2003, **118**, 1620–1633.
38 L. Jensen, M. Swart and P. Th. van Duijnen, *J. Chem. Phys.*, 2005, **122**, 034103.
39 L. Jensen and P. Th. van Duijnen, *Int. J. Quantum Chem.*, 2005, **102**, 612–619.
40 L. Jensen and P. Th. van Duijnen, *J. Chem. Phys.*, 2005, **123**, 074307.
41 T. A. Wesolowski and A. Warshel, *J. Phys. Chem.*, 1993, **97**, 8050–8053.
42 T. A. Wesolowski, in *Computational Chemistry: Reviews of Current Trends*, ed. J. Leszczynski, World Scientific, Singapore, 2006, vol. XI.
43 J. Neugebauer, Ch. R. Jacob, T. A. Wesolowski and E. J. Baerends, *J. Phys. Chem. A*, 2005, **109**, 7805–7814.
44 J. Neugebauer, M. J. Louwerse, P. Belanzoni, T. A. Wesolowski and E. J. Baerends, *J. Chem. Phys.*, 2005, **123**, 114101.
45 J. Kongsted, A. Osted, K. V. Mikkelsen and O. Christiansen, *Chem. Phys. Lett.*, 2002, **364**, 379–386.
46 T. A. Wesolowski, H. Chermette and J. Weber, *J. Chem. Phys.*, 1996, **105**, 9182–9190.
47 T. A. Wesolowski, *J. Chem. Phys.*, 1997, **106**, 8516–8526.
48 T. A. Wesolowski, Y. Ellinger and J. Weber, *J. Chem. Phys.*, 1998, **108**, 6078–6083.
49 A. Lembarki and H. Chermette, *Phys. Rev. A*, 1994, **50**, 5328–5331.
50 T. Wesolowski and A. Warshel, *J. Phys. Chem.*, 1994, **98**, 5183–5187.

51 T. A. Wesolowski and J. Weber, *Chem. Phys. Lett.*, 1996, **248**, 71–76.
52 M. E. Casida and T. A. Wesolowski, *Int. J. Quantum Chem.*, 2004, **96**, 577–588.
53 T. A. Wesolowski, *J. Am. Chem. Soc.*, 2004, **126**, 11444–11445.
54 L. Jensen, P.-O. Åstrand, K. O. Sylvester-Hvid and K. V. Mikkelsen, *J. Phys. Chem. A*, 2000, **104**, 1563–1569.
55 L. Jensen, P.-O. Åstrand, A. Osted, J. Kongsted and K. V. Mikkelsen, *J. Chem. Phys.*, 2002, **116**, 4001–4010.
56 B. Thole, *Chem. Phys.*, 1981, **59**, 341–350.
57 P. Th. van Duijnen and M. Swart, *J. Phys. Chem. A*, 1998, **102**, 2399–2407.
58 ADF, Amsterdam density functional program, Theoretical Chemistry, Vrije Universiteit Amsterdam, http://www.scm.com, 2005.
59 G. te Velde, F. M. Bickelhaupt, E. J. Baerends, C. Fonseca Guerra, S. J. A. van Gisbergen, J. G. Snijders and T. Ziegler, *J. Comput. Chem.*, 2001, **22**, 931–967.
60 P. R. T. Schipper, O. V. Gritsenko, S. J. A. van Gisbergen and E. J. Baerends, *J. Chem. Phys.*, 2000, **112**, 1344–1352.
61 O. V. Gritsenko, P. R. T. Schipper and E. J. Baerends, *Chem. Phys. Lett.*, 1999, **302**, 199–207.
62 O. V. Gritsenko, P. R. T. Schipper and E. J. Baerends, *Int. J. Quantum Chem.*, 2000, **76**, 407–419.
63 Ch. R. Jacob, T. A. Wesolowski and L. Visscher, *J. Chem. Phys.*, 2005, **123**, 174104.
64 A. D. Becke, *Phys. Rev. A*, 1988, **38**, 3098–3100.
65 J. P. Perdew, J. A. Chevary, S. H. Vosko, K. A. Jackson, M. R. Pederson, D. J. Singh and C. Fiolhais, *Phys. Rev. B*, 1992, **46**, 6671–6687.
66 S. J. A. van Gisbergen, J. G. Snijders and E. J. Baerends, *Comput. Phys. Commun.*, 1999, **118**, 119–138.
67 S. J. A. van Gisbergen, J. G. Snijders and E. J. Baerends, *J. Chem. Phys.*, 1995, **103**, 9347–9354.
68 *CRC Handbook of Chemistry and Physics*, ed. D. R. Lide, CRC, Boca Raton, FL, 78th edn, 1998.
69 M. B. Robin, *Higher Excited States of Polyatomic Molecules*, Academic Press, New York, 1975, vol. I.
70 M. B. Robin, *Higher Excited States of Polyatomic Molecules*, Academic Press, New York, 1985, vol. III.
71 G. D. Kerr, R. N. Hamm, M. W. Williams, R. D. Birkhoff and L. R. Painter, *Phys. Rev. A*, 1972, **5**, 2523–2527.
72 O. Christiansen, T. M. Nymand and K. V. Mikkelsen, *J. Chem. Phys.*, 2000, **113**, 8101–8112.
73 M. Grüning, O. V. Gritsenko, S. J. A. van Gisbergen and E. J. Baerends, *J. Chem. Phys.*, 2002, **116**, 9591–9601.
74 J. Neugebauer, E. J. Baerends and M. Nooijen, *J. Chem. Phys.*, 2004, **121**, 6155–6166.
75 G. Maroulis, *Chem. Phys. Lett.*, 1998, **289**, 403–411.
76 A. J. Russel and M. A. Spackmann, *Mol. Phys.*, 1995, **84**, 1239–1255.